Available online at www.sciencedirect.com

ScienceDirect

Mendeleev Commun., 2024, **34**, 325–328

Mendeleev Communications

Phenyl substitution as an effective way to control the luminescent properties of polyphenylcyclopentadienyl lanthanide complexes

Lada N. Puntus,[a,b] Daniil A. Bardonov,[a,c] Evgenia A. Varaksina,[a,d] Ilya V. Taydakov,[a,d] Dmitrii M. Roitershtein,*[a,e] Ilya E. Nifant'ev[a,f] and Konstantin A. Lyssenko[f,g]

[a] *A. V. Topchiev Institute of Petrochemical Synthesis, Russian Academy of Sciences, 119991 Moscow, Russian Federation. E-mail: roiter@yandex.ru*
[b] *V. A. Kotelnikov Institute of Radioengineering and Electronics, Russian Academy of Sciences, 141190 Fryazino, Moscow Region, Russian Federation*
[c] *National Research University Higher School of Economics (HSE University), 101000 Moscow, Russian Federation*
[d] *P. N. Lebedev Physical Institute, Russian Academy of Sciences, 119991 Moscow, Russian Federation*
[e] *N. D. Zelinsky Institute of Organic Chemistry, Russian Academy of Sciences, 119991 Moscow, Russian Federation*
[f] *Department of Chemistry, M. V. Lomonosov Moscow State University, 119991 Moscow, Russian Federation*
[g] *G. V. Plekhanov Russian University of Economics, 117997 Moscow, Russian Federation*

DOI: 10.1016/j.mencom.2024.04.005

Lanthanide complexes $[Cp^{X}LnCl_2(Me_3tach)]_n$ (Ln = Tb, Gd; Cp^{X} = Cp, Cp^{Ph_2}, Cp^{Ph_4}; Me_3tach = 1,3,5-trimethyl-1,3,5-triazacyclohexane; *n* = 1, 2), containing cyclopentadienyl (Cp), 1,3-diphenylcyclopentadienyl (Cp^{Ph_2}) and tetraphenylcyclopentadienyl (Cp^{Ph_4}) anions as π-bonded antenna ligands, have been synthesized. A combined analysis of quantum chemical, optical and X-ray diffraction data has shown that the introduction of phenyl groups into the Cp ring leads to the inevitable appearance of intraligand charge transfer states due to the nonequivalence of the phenyl rings.

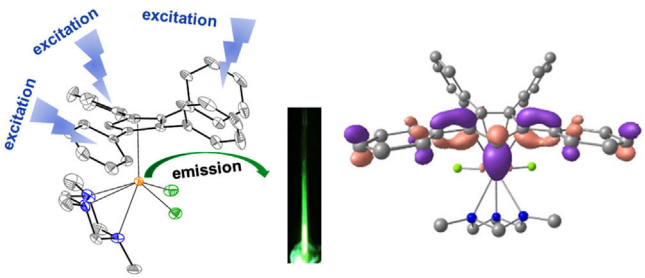

Keywords: lanthanide ions, luminescence, crystal structure, charge transfer state, cyclopentadienyl ligand.

The widespread use of lanthanides is based mainly on their ability to emit in various spectral regions (from visible to near-IR) with high luminescence quantum yields achieved due to the antenna effect.[1–4] One of the most common 'antenna' elements is the aromatic ring. Lanthanide complexes containing cyclopentadienyl as a π-bonded antenna have already shown themselves to be bright luminophores, but methods for predicting and tuning the luminescent properties of these systems have not yet been developed.[5–7] In particular, the introduction of N-heterocyclic ligands into lanthanide complexes containing triphenyl-substituted Cp ligands leads to strong luminescence quenching through the ligand-to-ligand charge transfer state. We therefore examined the roles of the number and degree of conjugation of phenyl groups attached to the Cp ligand. Obviously, it is desirable to reduce possible interligand interactions, which was achieved by the synthesis of mononuclear complexes in which the auxiliary ligand 1,3,5-trimethyl-1,3,5-triazacyclohexane (Me_3tach) fills the coordination sphere of the lanthanide ion. To elucidate the role of phenyl groups in the luminescence sensitization of the terbium ion, a complex with unsubstituted Cp was considered as a starting point. As a result, we have synthesized and structurally characterized complexes with both unsubstituted Cp and Cp containing two and four phenyl groups, and have analyzed their optical properties.

Cyclopentadienyl triazacyclohexane complexes $[CpLnCl_2(Me_3tach)]_2$ (Ln = Gd **1Gd** and Tb **1Tb**) can be obtained from the known cyclopentadienyl dichloride complexes $[CpLnCl_2(THF)_3]$[8] and Me_3tach (Scheme 1). The molecular structure of complex **1Gd** has been elucidated using X-ray diffraction (XRD) studies. Complex **1Gd** is a binuclear complex consisting of two equivalent fragments {CpGdCl(Me_3tach)} bridged by two chloride ligands. The two halves of the complex are oriented to maximize the distance between the bulkier Me_3tach ligands.

Heteroleptic complexes with di- and tetraphenylcyclopentadienyl ligands, $[Cp^{Ph_2}LnCl_2(Me_3tach)]$ (Ln = Gd **2Gd** and Tb **2Tb**, Cp^{Ph_2} = 1,3-diphenylcyclopentadienyl) and $[Cp^{Ph_4}LnCl_2(Me_3tach)]$ (Ln = Gd **3Gd** and Tb **3Tb**, Cp^{Ph_4} = tetraphenylcyclopentadienyl), were prepared *in situ* from Me_3tach and monocyclopentadienyl halide complexes, which in turn were obtained from $LnCl_3(THF)_x$ and potassium di- or tetraphenylcyclopentadienides (Scheme 2). The structures of complexes **2Ln** and **3Ln** were also determined by X-ray

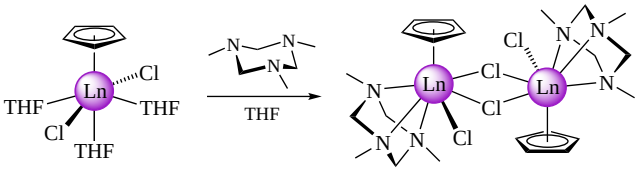

1Gd Ln = Gd
1Tb Ln = Tb

Scheme 1

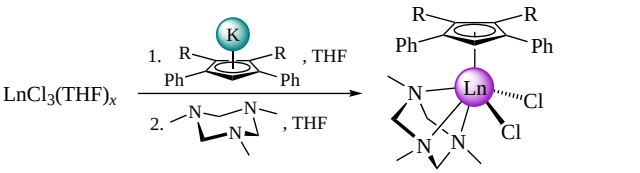

2Gd R = H, Ln = Gd **3Gd** R = Ph, Ln = Gd
2Tb R = H, Ln = Tb **3Tb** R = Ph, Ln = Tb

Scheme 2

crystallography. Complexes **2Ln** and **3Ln** have a structure similar to our previously described terbium complex $[Cp^{Ph_3}TbCl_2(Me_3tach)]$ (Cp^{Ph_3} = 1,2,4-triphenylcyclopentadienyl).[5]

According to XRD data,† the phenyl-substituted cyclopentadienyl complexes **2Ln** and **3Ln** are mononuclear, while complex **1Gd** crystallizes as a dimer with two μ_2-chloride anions (Figure 1). In both pairs, complexes **2Gd** and **2Tb**, as well as **3Gd** and **3Tb**, are isostructural. Assuming that complexes **3Ln** crystallize in the chiral space group $P2_1$, one should expect the presence of triboluminescence for the Tb complex. Although the geometry of complexes **1Ln**–**3Ln** is rather expected, there are a number of characteristics that are important for further analysis. First, the Ln–centroid distances ($Ln–Cp_{cent}$) in complexes **1Ln** and **2Ln** are equal to each other (for complexes **1Gd** and **2Gd** they are 2.41 Å). It should be noted that the observed $Ln–Cp_{cent}$ values for complexes with Me_3tach are

† *Crystal data for* **1Gd**. $C_{22}H_{40}N_6Cl_4Gd_2$ (M = 844.90), orthorhombic, space group *Pbca*, Z = 4, T = 100 K, a = 13.503(4), b = 14.213(4) and c = 15.534(3) Å, V = 2981.3(13) Å^3. A total of 9930 reflections ($2\theta_{max}$ = 50°) were collected, and 2619 independent reflections were used for the structure solution and refinement, which converged to R_1 = 0.0514 (for 1628 observed reflections), wR_2 = 0.1604, GOF = 0.873.

Crystal data for **2Gd**. $C_{23}H_{28}Cl_2GdN_3$ (M = 574.63), monoclinic, space group $P2_1/c$, Z = 4, T = 120 K, a = 18.0801(10), b = 9.4751(5) and c = 14.5494(8) Å^3, β = 110.846(2)°, V = 2329.3(2) Å^3. A total of 33291 reflections ($2\theta_{max}$ = 58°) were collected, and 6191 independent reflections were used for the structure solution and refinement, which converged to R_1 = 0.0394 (for 4706 observed reflections), wR_2 = 0.0824, GOF = 1.039.

Crystal data for **2Tb**. $C_{23}H_{28}Cl_2TbN_3$ (M = 576.30), monoclinic, space group $P2_1/c$, Z = 4, T = 120 K, a = 18.0670(19), b = 9.4724(14) and c = 14.5515(16) Å, β = 110.898(3)°, V = 2326.5(5) Å^3. A total of 17113 reflections ($2\theta_{max}$ = 55°) were collected, and 5333 independent reflections were used for the structure solution and refinement, which converged to R_1 = 0.0443 (for 4155 observed reflections), wR_2 = 0.1031, GOF = 0.953.

Crystal data for **3Gd**. $C_{41}H_{48}Cl_2GdN_3O_{1.50}$ (M = 834.97), monoclinic, space group $P2_1$, Z = 4, T = 120 K, a = 10.4547(6), b = 14.2173(7) and c = 25.8479(12) Å, β = 98.039(2)°, V = 3804.2(3) Å^3. A total of 32350 reflections ($2\theta_{max}$ = 54°) were collected, and 14825 independent reflections were used for the structure solution and refinement, which converged to R_1 = 0.0475 (for 13599 observed reflections), wR_2 = 0.0994, GOF = 1.023.

Crystal data for **3Tb**. $C_{41}H_{48}Cl_2TbN_3O_{1.50}$ (M = 836.64), monoclinic, space group $P2_1$, Z = 4, T = 120 K, a = 10.4328(9), b = 14.2211(10) and c = 25.8297(18) Å, β = 97.969(3)°, V = 3795.2(5) Å^3. A total of 32322 reflections ($2\theta_{max}$ = 54°) were collected, and 16327 independent reflections were used for the structure solution and refinement, which converged to R_1 = 0.0521 (for 14200 observed reflections), wR_2 = 0.1093, GOF = 0.975.

The measurements were performed using a Bruker D8 QUEST diffractometer (MoK_α radiation, ω- and φ-scans technique). The structures were solved by dual methods and refined in the anisotropic displacement model.

CCDC 2311250–2311254 contain the supplementary crystallographic data for this paper. These data can be obtained free of charge from The Cambridge Crystallographic Data Centre *via* http://www.ccdc.cam.ac.uk.

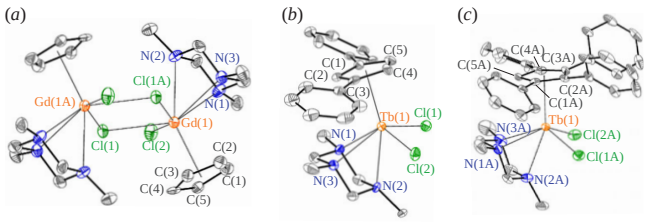

Figure 1 Molecular structures of (*a*) complex **1Gd**, (*b*) complex **2Tb** and (*c*) complex **3Tb** with atomic displacement parameters at 50% probability level. All hydrogen atoms are omitted for clarity.

systematically shorter than those for similar complexes containing three coordinated THF molecules. For example, for complex **2Tb** and its THF analog $[Cp^{Ph_2}TbCl_2(THF)_3]$,[5(*a*)] the decrease in the corresponding distance is 0.035 Å. The latter value coincides with the increase in $Tb–Cp_{cent}$ in complex **3Tb** (2.43–2.44 Å, two independent molecules in the unit cell) compared to complex **2Tb**. A comparison of the geometry of the π-antenna ligands in complexes **2Tb** and **3Tb** clearly shows that at least two phenyl rings in complex **3Tb** are characterized by rotation angles (26.5–37.8°) coinciding with those in complex **2Tb**. The residual dihedral angles of the phenyl groups in complex **3Tb** are quite far from the optimal values for conjugation and are in the range of 52.3–73.8°. Summarizing, the difference in the $Ln–Cp_{cent}$ distances in complexes **1Ln**–**3Ln** is mainly due to steric effects.

All the designed complexes were investigated by optical spectroscopy. The luminescence spectra of the Tb complexes exhibit characteristic narrow emission bands assigned to the $4f^8$–$4f^8$ transitions of the Tb^{3+} ion (Figure 2). The type of splitting pattern of the $^5D_4 \rightarrow {}^7F_J$ (J = 6–0) transitions is similar in complexes **1Tb** and **3Tb**, but different from that in complex **2Tb**. To assess the asymmetry of the ligand field, the branching ratio (β) is generally used,[5] which is the ratio of the integral intensity of the $^5D_4 \rightarrow {}^7F_6$ ($\Delta J = 2$) transition to that of the $^5D_4 \rightarrow {}^7F_5$ ($\Delta J = 1$) transition (Table 1). It is worth to mention that the most symmetrical nearest surrounding of the Tb ion is observed in complex **2Tb**, but at room temperature the value of β increases significantly (0.21 *vs.* 0.31, respectively). Such changes in the luminescence spectra may be caused by a phase transition in complex **2Tb**. The luminescence decay of the Tb complexes was fitted to a monoexponential function, which confirms the presence of only one luminescence center. It was found that the $^5D_4$ lifetimes of complexes **1Tb** and **3Tb** are essentially independent of temperature, thereby reflecting the low

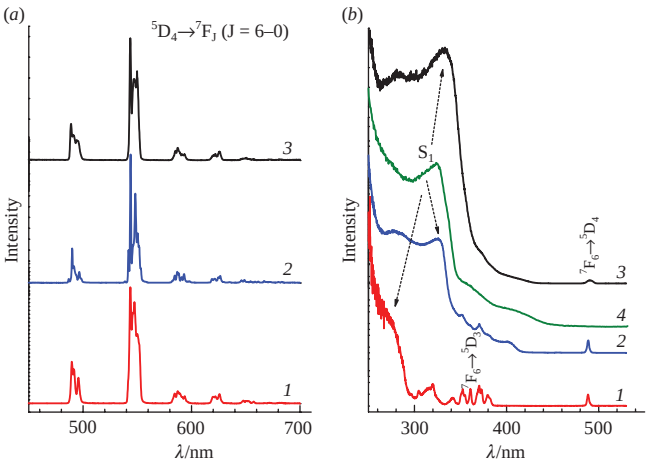

Figure 2 (*a*) Luminescence and (*b*) luminescence excitation spectra of (*1*) complex **1Tb**, (*2*) complex **2Tb** and (*3*) complex **3Tb** at T = 77 K (λ_{ex} = 280 nm, λ_{reg} = 545 nm). Green curve *4* is the excitation spectrum of complex **2Gd**.

Table 1 The observed lifetimes of the $^5D_4$ level (τ_{obs}), branching ratio (β), energy (E) of S_1 and T states, energy gaps (E_1 and E_2) and overall quantum yield (Q_{Tb}^{Lig}) for the Tb complexes.

Complex	τ_{obs}/ms		β	$E(S_1)$/ nm	E_1/ cm^{-1}	E(T)/ nm	E_2/ cm^{-1}	Q_{Tb}^{Lig} (%)
	300 K	77 K						
1Tb	0.54 ± 0.03	0.53 ± 0.02	0.26	275	10050	390	5815	13
2Tb	0.47 ± 0.02	0.41 ± 0.01	0.21	325	6675	415	3595	24
3Tb	0.46 ± 0.02	0.43 ± 0.02	0.31	330	6775	425	3030	35

probability of thermally activated nonradiative processes in contrast to complex **2Tb**.

The steady-state luminescence excitation spectra of the Tb complexes, monitored around the maximum of the intense $^5D_4 \rightarrow {}^7F_5$ transition of the Tb^{3+} ion at 545 nm, are presented in Figure 2. These spectra exhibit overlapping intense bands corresponding to π–π* transitions in the Cp ligand, as well as weak narrow bands corresponding to the $4f^8$ intraconfigurational transitions. According to previous studies of Ln complexes with the phenyl-substituted Cp ligand,[5] the energy of the S_1 state in the complexes under consideration is ~275, 325 and 330 nm in complexes **1Tb**, **2Tb** and **3Tb**, respectively. In the excitation spectra of complexes **2Tb** and **3Tb**, an additional broad band is observed in the region of 350–420 nm, as in the corresponding spectra of the Gd complexes (Figures 2 and S1, see Online Supplementary Materials). This band can be tentatively assigned to the intraligand charge transfer (ILCT) state. Earlier, a similar ILCT state was found in the excitation spectra of lanthanide complexes with phenyl-substituted Cp ligands, in which the K^+ cation participates in additional coordination with the phenyl rings of the Cp ligands.[5] A combined analysis of the spectral and structural data shows that the detected charge transfer state is due to the nonequivalence of the phenyl rings of the Cp ligand, which is consistent with the absence of these groups in complex **1Tb**. The overall quantum yield of photoluminescence is 13, 24 and 35% for complexes **1Tb**, **2Tb** and **3Tb**, respectively. The low value of Q_{Tb}^{Lig} in complex **1Tb** is due to the large difference between the energies of the singlet and triplet states: $E_1 = E(S_1) - E(T)$ and $E_2 = E(T) - E(^5D_4)$, 10725 and 5140 cm^{-1}, respectively. The phosphorescence spectra of the corresponding Gd complexes were examined and 0-phonon transitions in Cp ligands were taken as the T-state energy (see Table 1). Interestingly, the introduction of the Me_3tach ligand into complexes with phenyl-substituted Cp leads to an increase in the triplet state energy. Based on the experimental data, the energy gaps (E_1 and E_2) are closer to the optimal values[9] in complex **2Tb** (6675 and 3595 cm^{-1}, respectively), and the best correlation is observed for complex **3Tb** (6775 and 3030 cm^{-1}, respectively). On the one hand, the presented data indicate the dominant role of the energy of the triplet state in the efficient luminescence sensitization of the Tb ion. But on the other hand, this efficiency strongly depends on the distance between the Ln ion and the ligand (~$1/R^6$), while in complex **2Tb** the Tb–Cp_{cent} distance is 2.39 Å, and in complex **3Tb** a longer distance is found (2.43 Å). To understand the inverse dependence found for Q_{Tb}^{Lig}, we have performed the geometry optimization of the ground and first triplet states for complexes **2Tb** and **3Tb**.‡

First of all, it should be noted that although the calculated energies of the S_0–T_1 transitions for complexes **2Tb** and **3Tb**, in contrast to the experimental values, turned out to be the same (420 nm), it is close to the experimental values within 5 nm. The geometry optimization of the ground state leads to a slight increase in the Tb–Cp_{cent} bond length in the isolated state (2.436 and 2.459 Å, respectively) compared to the crystal, but the difference of these values for complexes **2Tb** and **3Tb** coincides with the experimental values (2.39–2.43 Å). Considering that the triplet state of the ligand plays an important role in luminescence sensitization, our attention was focused on the geometry of the latter. Optimization of the T_1 state showed that excitation causes ring slippage towards the unsubstituted carbon atom in Cp, the C(2) atom in complex **2Tb** and the C(5) atom in complex **3Tb** (see Figure 1). A significant decrease in the distance to the indicated carbon atoms C(2) or C(5) is observed, which is even slightly shorter for complex **3Tb** (2.56 Å) than for complex **2Tb** (2.58 Å). For comparison, the remaining carbon atoms of the Cp ring in complexes **2Tb** and **3Tb** form significantly longer bonds of 2.76–2.78 and 2.76–2.88 Å, respectively. This difference in the length of the Tb–C bonds also causes some distortion of the planarity of the Cp ring, which is expressed in the deviation of one of the carbon atoms by 0.13 Å from the plane. Another interesting feature is that in complex **3Tb** there is a significant decrease in the dihedral angles between the first and fourth Ph groups and the Cp ring from 31° in the ground state to 21° in the excited state. Apparently, this effect is due to a decrease in steric repulsion upon distortion of the complex in the triplet state. For comparison, in complex **2Tb** the corresponding values in the ground and excited states are 26° and 22°, respectively. Thus, in the triplet state, the degree of overlap between the antenna π-system and the Tb ion is equalized to some extent. The similarity of geometry in the triplet state of complexes **2Tb** and **3Tb** eliminates the controversy between the geometry and the efficiency of the luminescence sensitization of the Tb^{3+} ion. Moreover, as can be seen from the excitation spectra, the efficiency of excitation of the Tb ion through the absorption bands of the ligand is significantly higher in complex **3Tb** than in complex **2Tb**, which is consistent with the found changes in the calculated geometry of complex **3Tb** in the triplet state.

Thus, the analysis of the presented optical and structural data shows that the introduction of phenyl groups into the Cp ring leads to the inevitable appearance of an intraligand charge transfer state as an intrinsic property of the π-bonded antenna Cp ligand. Depending on a number of factors such as the energies of the excited states, the steric overcrowding of the system and its supramolecular organization, this state can be useful for increasing the efficiency of luminescence sensitization of the lanthanide ion. The degree of overlap between the π-system of the Cp ligand and the lanthanide ion can be controlled by the introduction of auxiliary ligands such as Me_3tach, but the ground state geometry reflects this only to a certain extent. Since the energy of the triplet state of the ligand plays an important role in luminescence sensitization, the geometry of the triplet state should also be considered in the design of lanthanide complexes with predetermined luminescent properties.

This research was supported by the Russian Science Foundation (grant no. 22-13-00312). The authors acknowledge the support of Lomonosov Moscow State University Program of Development in providing access to single-crystal X-ray diffraction.

‡ Optimizations for the ground singlet and first triplet states of complexes **2Tb** and **3Tb** were carried out using the hybrid PBE functional and large-core energy-adjusted RECPs for Tb, developed by the Stuttgart and Dresden groups, along with the accompanying basis set ECP54MWB to describe the valence electron density.[10,11] Large-core energy-adjusted RECPs for the lanthanides put the 5*s*, 5*p*, 6*d* and 6*s* shells in the valence space, whereas the 4*f* electrons belonged to the core pseudopotentials. For the other atoms, the 6-311+g* basis set was used. The calculations always used tight SCF convergence and standard optimization convergence criteria along with ultrafine grids. All calculations were performed using the G09 program package.[12]

Online Supplementary Materials

Supplementary data associated with this article can be found in the online version at doi: 10.1016/j.mencom.2024.04.005.

References

1 J.-C. G. Bünzli, *Acc. Chem. Res.*, 2006, **39**, 53.
2 S. V. Eliseeva and J.-C. G. Bünzli, *New J. Chem.*, 2011, **35**, 1165.
3 S. V. Eliseeva and J.-C. G. Bünzli, *Chem. Soc. Rev.*, 2010, **39**, 189.
4 *Luminescence of Lanthanide Ions in Coordination Compounds and Nanomaterials*, ed. A. de Bettencourt-Dias, John Wiley & Sons, Ltd., Chichester, UK, 2014.
5 (*a*) D. M. Roitershtein, L. N. Puntus, A. A. Vinogradov, K. A. Lyssenko, M. E. Minyaev, M. D. Dobrokhodov, I. V. Taidakov, E. A. Varaksina, A. V. Churakov and I. E. Nifant'ev, *Inorg. Chem.*, 2018, **57**, 10199; (*b*) D. A. Bardonov, P. D. Komarov, V. I. Ovchinnikova, L. N. Puntus, M. E. Minyaev, I. E. Nifant'ev, K. A. Lyssenko, V. M. Korshunov, I. V. Taidakov and D. M. Roitershtein, *Organometallics*, 2021, **40**, 1235; (*c*) D. A. Bardonov, L. N. Puntus, I. V. Taidakov, E. A. Varaksina, K. A. Lyssenko, I. E. Nifant'ev and D. M. Roitershtein, *Mendeleev Commun.*, 2022, **32**, 198.
6 (*a*) J.-C. G. Bünzli, in *Handbook on the Physics and Chemistry of Rare Earths*, eds. J.-C. G. Bünzli and V. K. Pecharsky, Elsevier, Amsterdam, 2016, vol. 50, pp. 141–176; (*b*) J.-C. G. Bünzli, *Coord. Chem. Rev.*, 2015, **293**–**294**, 19.
7 (*a*) J.-C. G. Bünzli, *Eur. J. Inorg. Chem.*, 2017, 5058; (*b*) I. F. Costa, L. Blois, T. B. Paolini, I. P. Assunção, E. E. S. Teotonio, M. C. F. C. Felinto, R. T. Moura, Jr., R. L. Longo, W. M. Faustino, L. D. Carlos, O. L. Malta, A. N. Carneiro Neto and H. F. Brito, *Coord. Chem. Rev.*, 2024, **502**, 215590.
8 S. Manastyrskyj, R. E. Maginn and M. Dubeck, *Inorg. Chem.*, 1963, **2**, 904.
9 M. Latva, H. Takalo, V.-M. Mukkala, C. Matachescu, J. C. Rodríguez-Ubis and J. Kankare, *J. Lumin.*, 1997, **75**, 149.
10 M. Dolg, H. Stoll, A. Savin and H. Preuss, *Theor. Chim. Acta*, 1989, **75**, 173.
11 M. Dolg, H. Stoll and H. Preuss, *Theor. Chim. Acta*, 1993, **85**, 441.
12 M. J. Frisch, G. W. Trucks, H. B. Schlegel, G. E. Scuseria, M. A. Robb, J. R. Cheeseman, G. Scalmani, V. Barone, G. A. Petersson, H. Nakatsuji, X. Li, M. Caricato, A. Marenich, J. Bloino, B. G. Janesko, R. Gomperts, B. Mennucci, H. P. Hratchian, J. V. Ortiz, A. F. Izmaylov, J. L. Sonnenberg, D. Williams-Young, F. Ding, F. Lipparini, F. Egidi, J. Goings, B. Peng, A. Petrone, T. Henderson, D. Ranasinghe, V. G. Zakrzewski, J. Gao, N. Rega, G. Zheng, W. Liang, M. Hada, M. Ehara, K. Toyota, R. Fukuda, J. Hasegawa, M. Ishida, T. Nakajima, Y. Honda, O. Kitao, H. Nakai, T. Vreven, K. Throssell, J. A. Montgomery, Jr., J. E. Peralta, F. Ogliaro, M. Bearpark, J. J. Heyd, E. Brothers, K. N. Kudin, V. N. Staroverov, T. Keith, R. Kobayashi, J. Normand, K. Raghavachari, A. Rendell, J. C. Burant, S. S. Iyengar, J. Tomasi, M. Cossi, J. M. Millam, M. Klene, C. Adamo, R. Cammi, J. W. Ochterski, R. L. Martin, K. Morokuma, O. Farkas, J. B. Foresman and D. J. Fox, *Gaussian 09*, Gaussian, Inc., Wallingford, CT, 2016.

Received: 5th December 2023; Com. 23/7331